

Supplementary Information

Computer-Aided Discovery of Novel Ebola Virus Inhibitors

Stephen J. Capuzzi^{1#}, Wei Sun^{2#}, Eugene N. Muratov^{1,3}, Carles Martínez-Romero^{4,5}, Gregory Tawa², Ethan G. Fisher², Miao Xu², Paul Shinn², Adolfo García-Sastre^{4,5,6}, Wei Zheng^{2*} and Alexander Tropsha^{1*}.

¹ *Laboratory for Molecular Modeling, Division of Chemical Biology and Medicinal Chemistry, UNC Eshelman School of Pharmacy, University of North Carolina at Chapel Hill, Chapel Hill, NC, 27599, USA.*

² *National Center for Advancing Translational Sciences, National Institutes of Health, Bethesda, MD 20892, USA.*

³ *Department of Chemical Technology, Odessa National Polytechnic University, Odessa, 65000, Ukraine.*

⁴ *Department of Microbiology, Icahn School of Medicine at Mount Sinai, New York, NY 10029, USA.*

⁵ *Global Health and Emerging Pathogens Institute, Icahn School of Medicine at Mount Sinai, New York, NY 10029, USA.*

⁶ *Department of Medicine, Division of Infectious Diseases, Icahn School of Medicine at Mount Sinai, New York, NY 10029, USA*

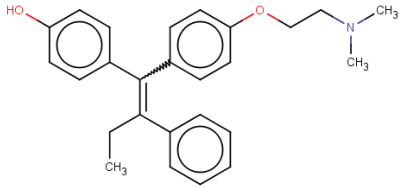
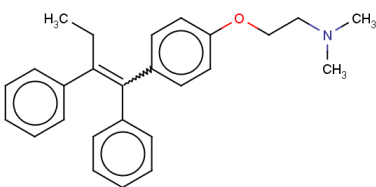
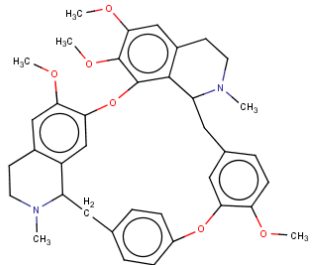
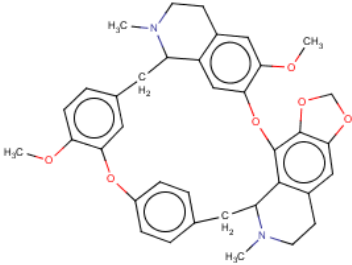
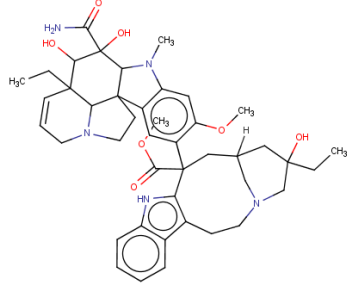
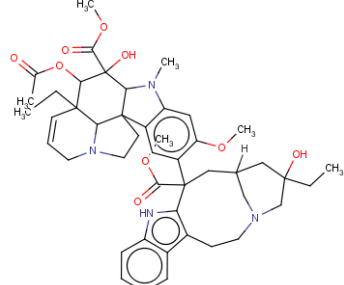
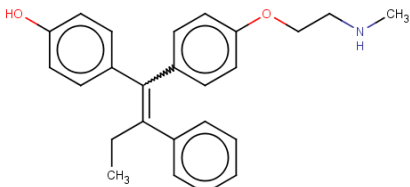
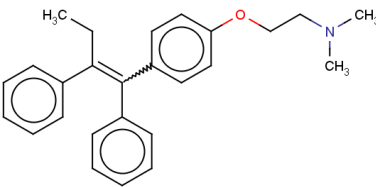
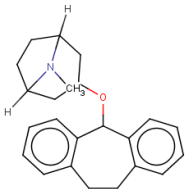
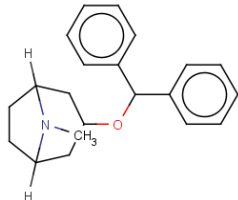
Table of Contents

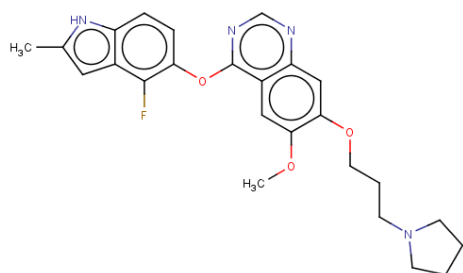
| | |
|-------------------------------------|-------|
| Supplementary Table 1 | S2 |
| Supplementary Table 2 | S3-S6 |
| Supplementary Figure 1 | S7 |
| Supplementary Figure 2 | S8 |
| Supplementary Figure 3 | S9 |
| Supplementary Figure 4 | S10 |
| Supplementary Figure 5 | S11 |

Supplementary Table 1. Statistical characteristics obtained on 5-fold external CV of all models developed in this study. The results with highest statistical metrics are highlighted in bold. HEK models built with Chembench and HiT QSAR were not used due to poor predictive power. Values below acceptance threshold are underlined.

| Model Name | Descriptors | MLT | CCR | SE | SP | PPV | NPV |
|------------------|-------------|---------|-------------|-------------|-------------|-------------|-------------|
| Chembench – P1 | Dragon 6.0 | RF | 0.67 | 0.69 | 0.68 | 0.66 | 0.68 |
| HiT QSAR – P1 | SiRMS | RF | 0.72 | 0.73 | 0.71 | 0.72 | 0.73 |
| GUSAR – P1 | MNA and QNA | SCR-RBF | 0.72 | 0.73 | 0.71 | 0.72 | 0.73 |
| Chembench – P2 | Dragon 6.0 | RF | 0.72 | 0.72 | 0.72 | 0.72 | 0.72 |
| HiT QSAR – P2 | SiRMS | RF | 0.75 | 0.75 | 0.75 | 0.75 | 0.75 |
| GUSAR – P2 | MNA and QNA | SCR-RBF | 0.72 | 0.69 | 0.75 | 0.73 | 0.71 |
| Chembench – HeLa | Dragon 6.0 | RF | 0.73 | 0.77 | 0.68 | 0.73 | 0.72 |
| HiT QSAR – HeLa | SiRMS | RF | 0.64 | 0.68 | 0.60 | 0.66 | 0.62 |
| GUSAR – HeLa | MNA and QNA | SCR-RBF | 0.75 | 0.67 | 0.84 | 0.82 | 0.69 |
| Chembench – HEK | Dragon 6.0 | RF | 0.62 | 0.67 | <u>0.57</u> | 0.64 | 0.60 |
| HiT QSAR – HEK | SiRMS | RF | <u>0.53</u> | <u>0.55</u> | <u>0.50</u> | <u>0.56</u> | <u>0.49</u> |
| GUSAR – HEK | MNA and QNA | SCR-RBF | 0.72 | 0.78 | 0.71 | 0.73 | 0.76 |

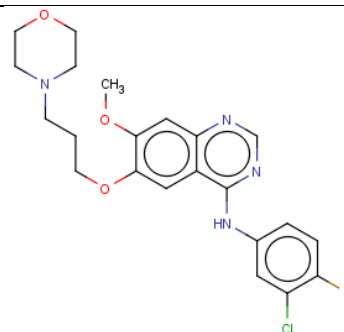
Supplementary Table 2. Structural similarity of top hits to training set compounds. The Tanimoto coefficient (T_C) between experimentally confirmed hits and compounds in the training set was calculated using ISIDA (see Methods). All neighbors from the training set were active according to both P1 and P2 definitions.

| Hit Name | Hit Structure | T_C | Training Set Compound | Compound Name |
|-------------|---|-------|---|---------------|
| Afimoxifene |  | 0.99 |  | Tamoxifen |
| Tetrandrine |  | 0.97 |  | Cepharanthine |
| Vindesine |  | 0.96 |  | Vinblastine |
| Endoxifen |  | 0.93 |  | Tamoxifen |
| Deptropine |  | 0.89 |  | Benztropine |

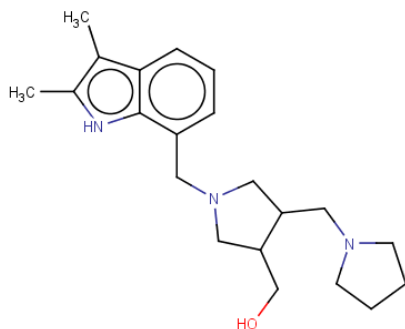


Cediranib

0.79

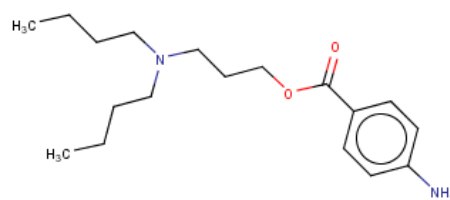


Gefitinib

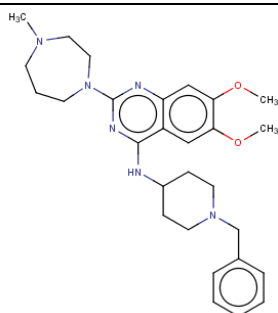


ZINC91973695

0.77

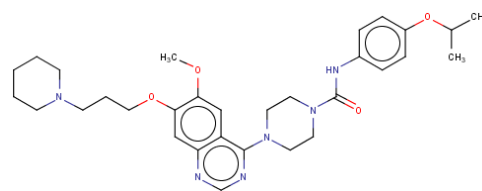


Butacaine

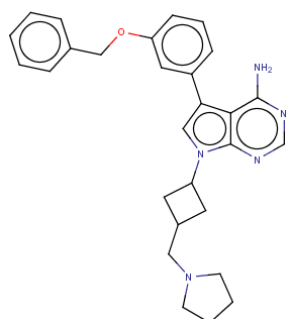


BIX-01294

0.75

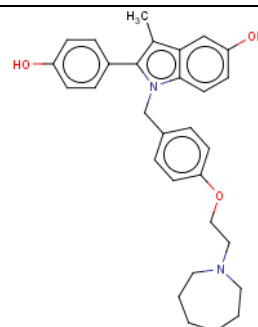


Tandutinib



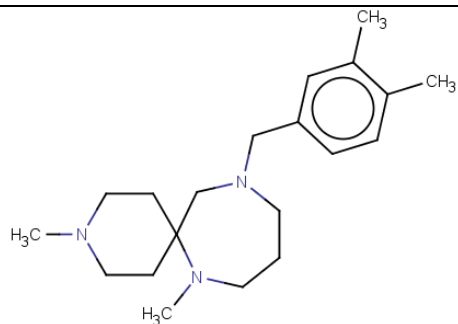
NVP-ADW742

0.72

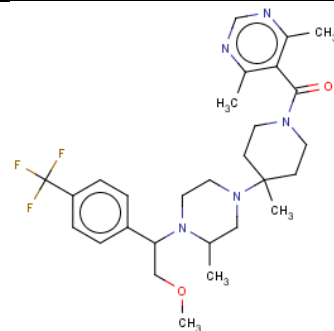


Bazedoxifene

ZINC67869167

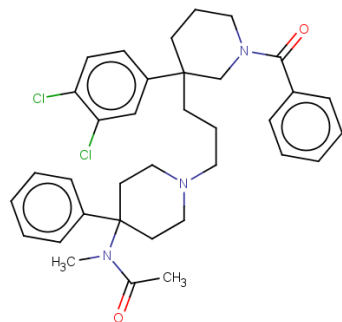


0.71

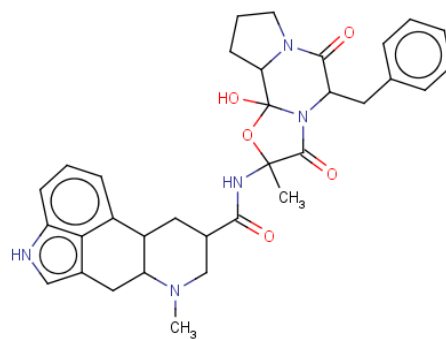


Vicriviroc

Osanetant

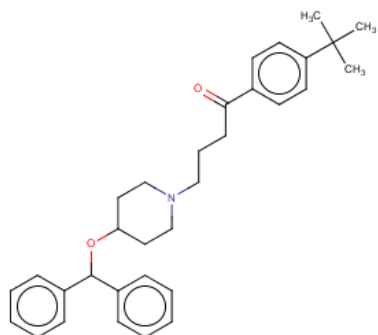


0.71

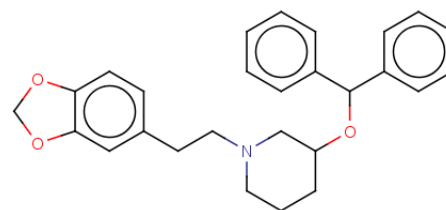


Dihydroergotamine

Ebastine

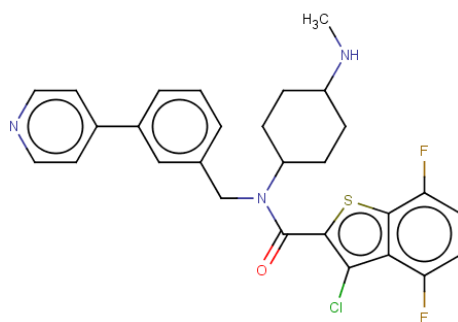


0.66

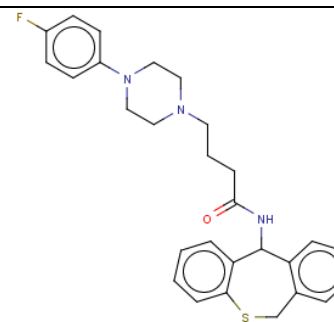


Zamifenacin

Hh-Ag1.5

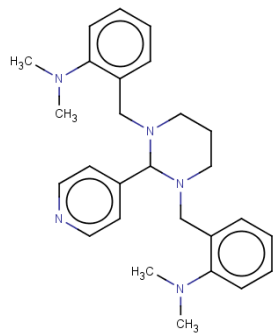


0.66

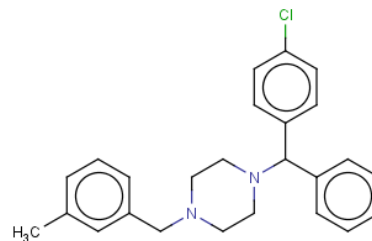


Monatepil

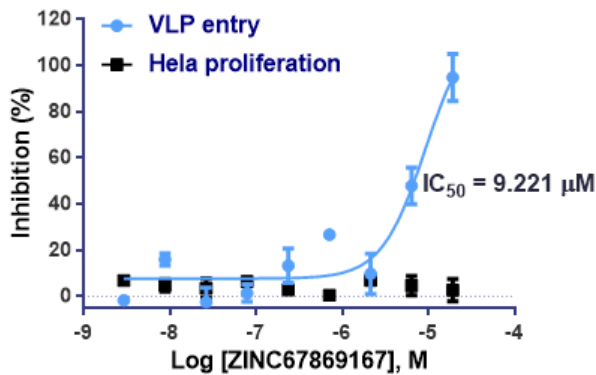
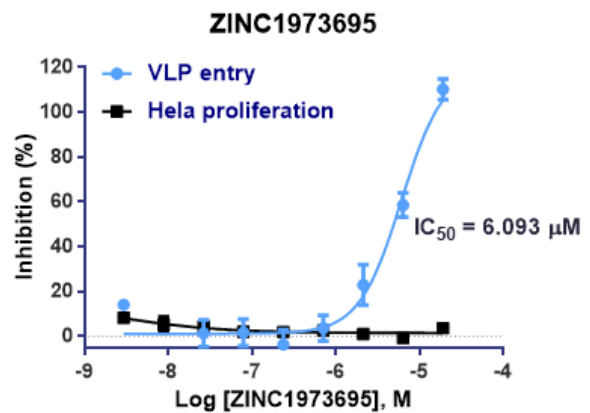
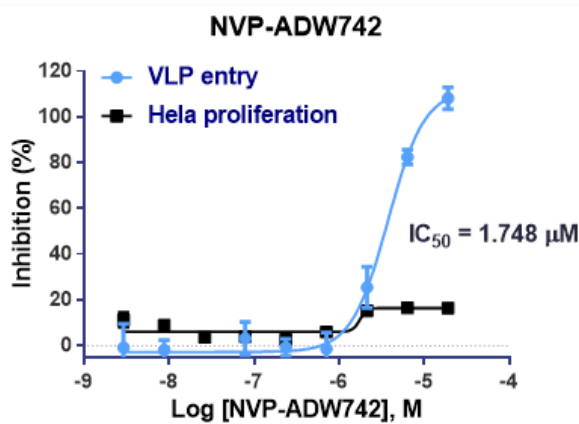
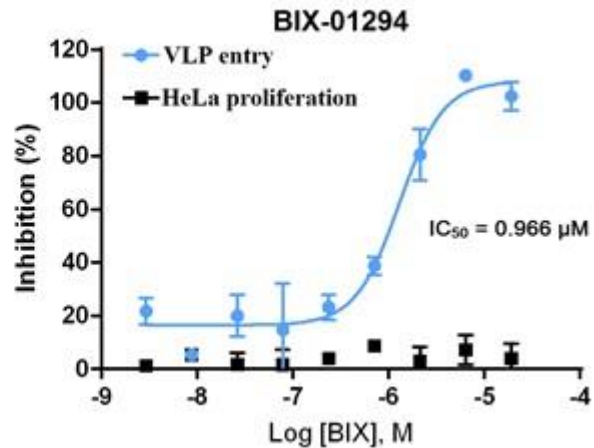
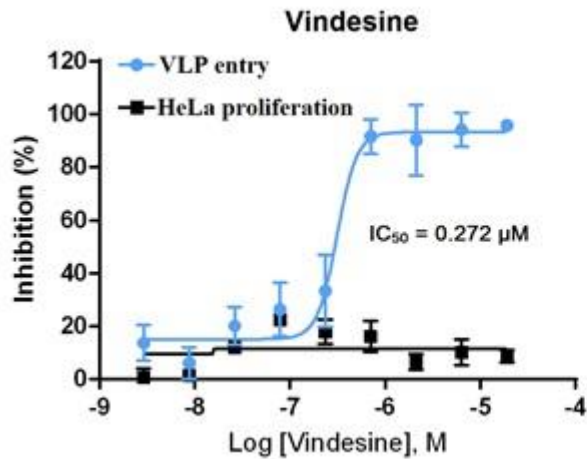
GANT61



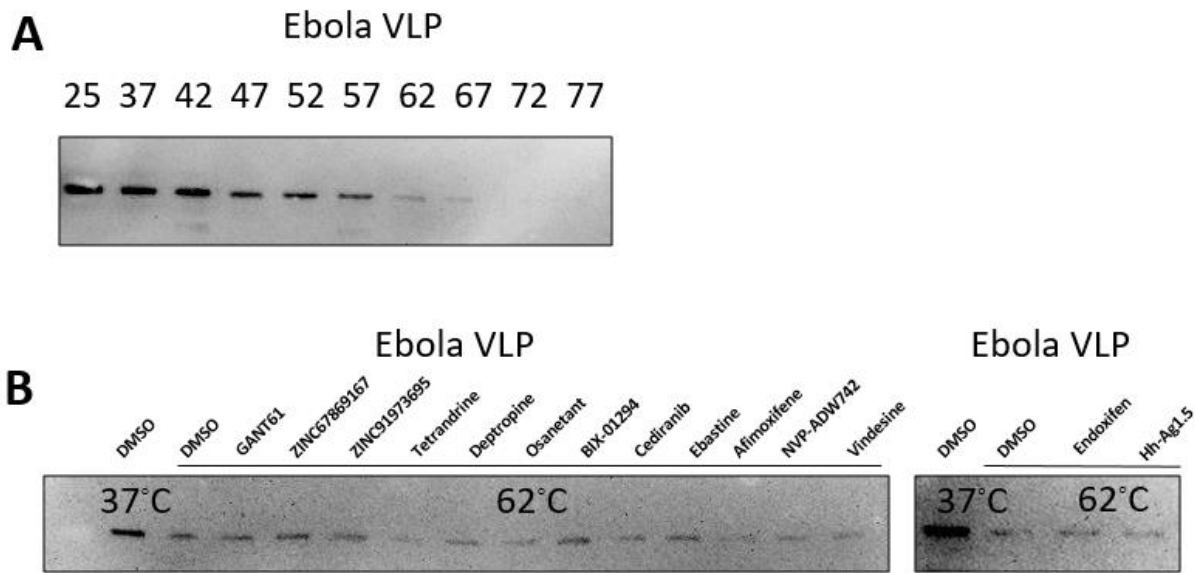
0.63



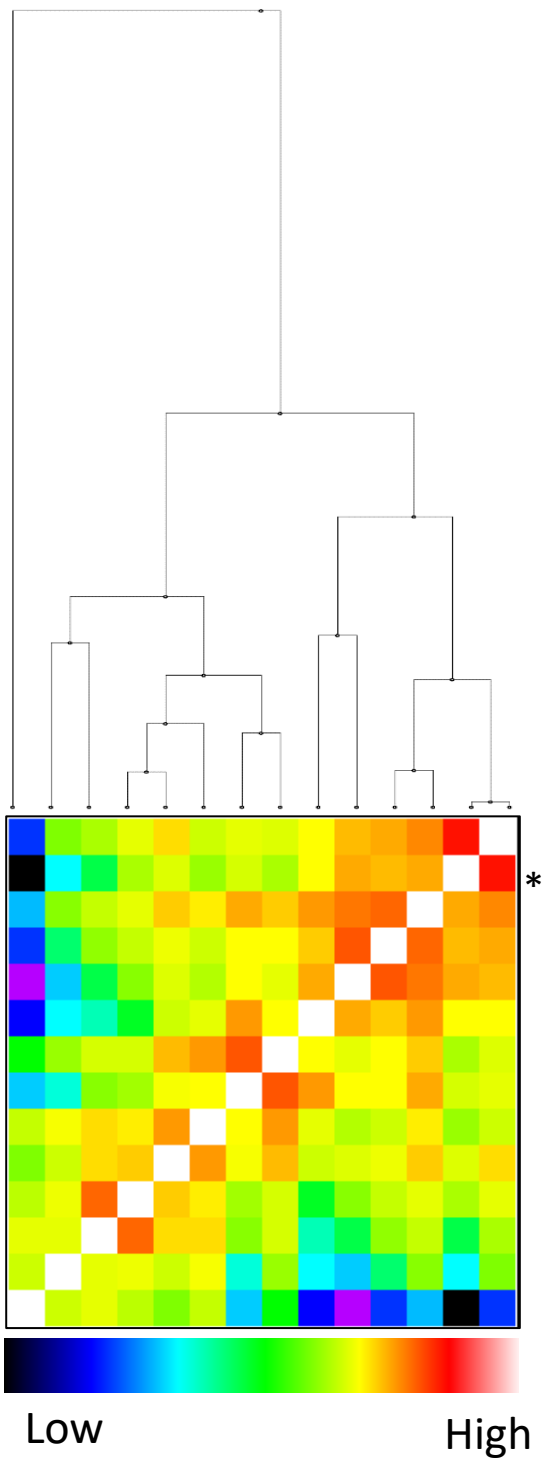
Meclizine



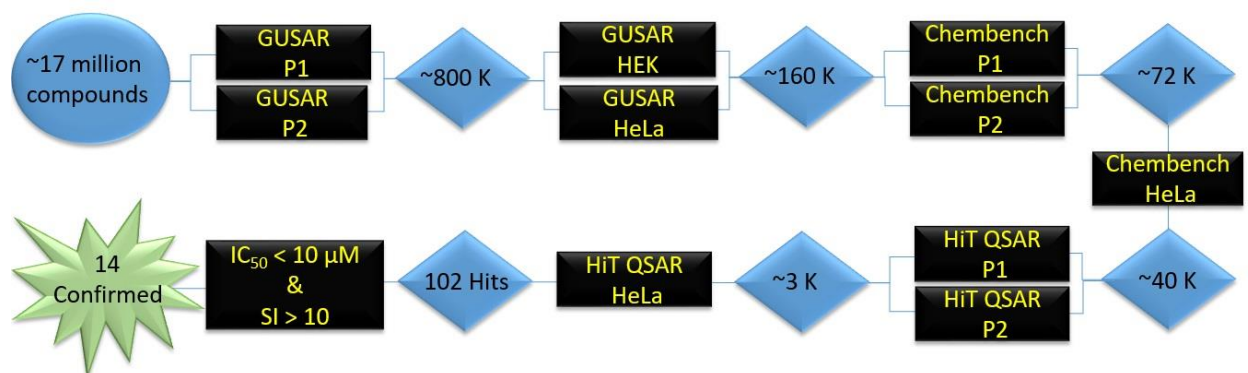
Supplementary Figure 1. Dose response curves for vindesine and BIX-01294. Both antiviral (VLP entry) and host cell cytotoxicity (HeLa) activities are plotted.



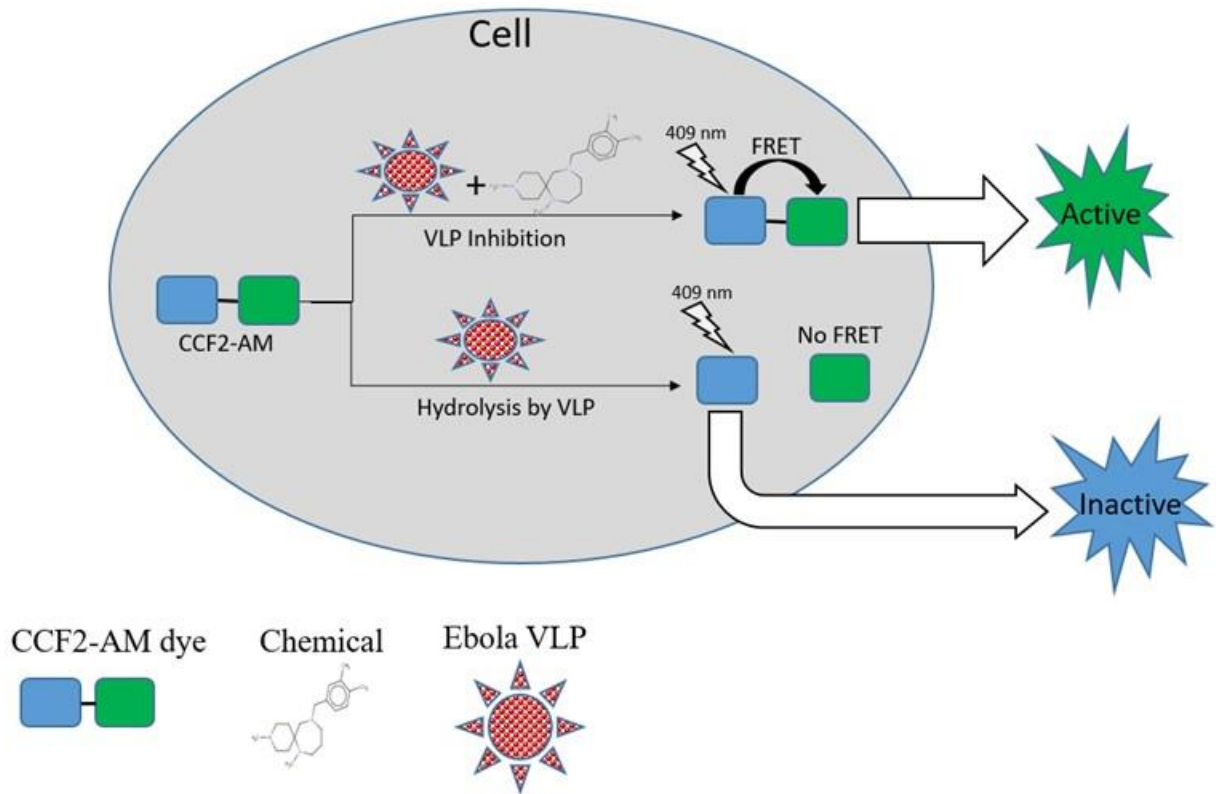
Supplementary Figure 2. Thermal profiling results of Ebola VLP with Ebola entry inhibitors. **A**, Thermal stability of Ebola VLP at temperatures from 25 °C to 77 °C detected by western blot. **B**, Effects of Ebola entry inhibitors (GANT61, ZINC67869167, ZINC91973695, tetrandrine, deptropine, osanetant, BIX-01294, cediranib, ebastine, afimoxifene, NVP-ADW742, vindesine, endoxifen, Hh-Ag1.5) on thermal stability of Ebola VLP at 62 °C. All experiments were performed in duplicate and data are representative of two independent experiments.



Supplementary Figure 3. Hierarchical clustering of experimental hits. High Tanimoto similarity of afimoxifene and endoxifen is highlighted by an asterisks.



Supplementary Figure 4. Screening workflow. A virtual chemical library of ~17 million compounds was screened against a battery of antiviral (P1 and P2) and cytotoxicity (HEK and HeLa) models. Hits selected for experimental validation were predicted to be EBOV inhibitors with limited host cytotoxicity. Then computational hits were experimentally validated, then their activity was evaluated using percent inhibition, IC_{50} values, and selectivity index (SI).



Supplementary Figure 5. Simplified schema of Ebola VLP assay. Ebola VLPs contain Ebola GP and the VP40 protein fused to a beta-lactamase (Bla) reporter. HeLa cells are loaded with the beta-lactamase substrate CCF2-AM. If the VLP enters into the cell, Bla hydrolyzes the substrate CCF2-AM, disrupting the fluorescence resonance energy transfer (FRET) in the substrate, thus causing blue fluorescence. Inhibition of the VLP by a chemical will preserve the substrate FRET, maintaining a green fluorescence. The ratio of blue/green fluorescence intensities represents the VLP activity of inside cells.